Valence Band X-Ray Emission Spectra of Compressed Germanium

Viktor V. Struzhkin,[1] Ho-kwang Mao,[1] Jung-Fu Lin,[1,*] Russell J. Hemley,[1] John S. Tse,[2,†] Yanming Ma,[2,‡]
Michael Y. Hu,[3] Paul Chow,[3] and Chi-Chang Kao[4]

[1]*Geophysical Laboratory, Carnegie Institution of Washington, 5251 Broad Branch Road NW, Washington, DC 20015, USA*
[2]*Steacie Institute for Molecular Science, National Research Council of Canada, 100 Sussex Drive, Ottawa, Ontario, Canada K1A 0R6*
[3]*HPCAT, Carnegie Institution of Washington, Advanced Photon Source, Argonne National Laboratory, Argonne, Illinois 60439, USA*
[4]*NSLS, Brookhaven National Laboratory, Upton, New York 11973, USA*

(Received 9 March 2004; revised manuscript received 3 March 2006; published 6 April 2006)

We report measurements of the valence band width in compressed Ge determined from x-ray emission spectra below the Ge *K* edge. The width of the valence band does not show any pressure dependence in the semiconducting diamond-type structure of Ge below 10 GPa. On the other hand, in the metallic β-Sn phase above 10 GPa the valence band width increases under compression. Density-functional calculations show an increasing valence band width under compression both in the semiconducting phase (contrary to experiment) and in the metallic β-Sn phase of Ge (in agreement with observed pressure-induced broadening). The pressure-independent valence band width in the semiconducting phase of Ge appears to require theoretical advances beyond the density-functional theory or the *GW* approximation.

DOI: 10.1103/PhysRevLett.96.137402 PACS numbers: 78.70.En , 61.10.Ht, 62.50.+p, 71.20.Mq

The bandwidth and the band gap may be considered as the most important parameter characterizing the electronic structure of a solid. Most band structure calculations available today are based on local approximation to density-functional theory (DFT) [1,2]. Even though Kohn-Sham eigenvalues [2] from that theory do not match exactly photoemission band-mapping experiments, they are remarkably similar to band energies obtained experimentally [3]. More exact quasiparticle (QP) calculations of band energies, which use Dyson's equation, include many-body corrections via the electron self-energy [3–10]. The predicted band broadening is only 0.05 eV in germanium and 0.08 eV in silicon [3,6] [both systems having $(4\pi\rho/3)^{-1/3} = r_s \sim 2.0$, where ρ is density of electrons]; i.e., the predicted effect is smaller than the typical uncertainty in a valence-band minimum determined by angle-resolved photoemission. On the other hand, the effect of pressure on the band gap in semiconductors is substantial [11] and should be easily detectable in the pressure range of diamond anvil cell (DAC) experiments. Unfortunately, photoemission measurements in DACs are not feasible. The alternative technique is to consider pressure effect on the valence-band emission line in Ge from $4p$ states to $1s$ core state [$K\beta_2$ at 11100.8 eV [12]], which is accessible using x-ray emission spectroscopy (XES) in DACs. The normal procedure for analyzing XES and x-ray absorption spectroscopy (XAS) assumes the final state rule [13], which means that the core-hole effects need to be taken into account for the XAS case, but not for the XES case. This is the reason why XES is more reliable if one wants to obtain density of states information directly. Such measurements are further motivated by the lack of consensus in theoretical models taking full account of many-body corrections to the band structure problem even in the case of simple metals [8,9,14,15], and by the scarce amount of experimental information regarding the pressure effects on the valence-band states. While the uniaxial pressure effects on the electronic states at the top of the valence band are quite well understood [16], the effects of pressure on the valence-band effective masses and on the electronic states deep in the valence band have been much less studied. The available experimental results on the binding energy of shallow impurity levels in Si [17] indicate that average effective mass of the valence band may even *decrease* under hydrostatic pressure, unexpectedly indicating possible *narrowing* of the valence band in compressed Si. On the contrary, the decrease of the effective mass of the conduction band is observed under compression in Si [17], which goes along with the expectations. The phase transitions at 10 GPa in Ge and at 12 GPa in Si are particularly interesting because of the possible change of electron-electron correlations between the semiconducting (insulator) and the metallic phase.

We report the valence-band emission studies of Ge through the phase transition at 10 GPa up to 31 GPa. We compare experimental results with theoretical calculations performed with the full potential linearized augmented plane wave method within the density-functional theory (DFT); the electrons exchange-correlation energy was described in the generalized gradient approximation (GGA). The experimentally determined width of the valence band is not increasing with pressure in the semiconducting diamond-type phase, contrary to theoretical results. The theoretical predictions for the metallic β-Sn phase above 10 GPa are in good agreement with experiment.

We have measured the valence-band x-ray emission spectra in compressed germanium at pressures between 1 to 31 GPa at the HPCAT inelastic x-ray scattering beam line (Advanced Photon Source, Argonne National Laboratory). A standard Mao-Bell piston-cylinder DAC with enlarged side openings was used in XES experiments. We used 300 μm flat culet diamonds. The Ge sample of

99.9999% purity was loaded into the hole about 50 μm in diameter drilled in a Be gasket (no pressure medium was used). The pressure in the sample chamber was measured using ruby fluorescence. The undulator gap was set at 13 keV (third harmonic). The monochromatic x-ray beam (1 eV FWHM) was focused down to 60 μm size at the sample position, and x-ray emission spectra were collected through the Be gasket. The signal level was about 300 cts/ sec with these settings. Figure 1 gives overview of measured spectra.

All calculations were performed with the full potential linearized augmented plane wave method using WIEN2K [18]. The electron exchange-correlation energy was described in the generalized gradient approximation [19]. The local-density approximation (LDA) [20] was also employed to compare with the GGA. The plane wave cutoff was set to RK max= 7.5. Convergence tests showed the use of 3000 k points for the calculation of the primitive unit cell in both diamond-type and β-Sn phases in the Brillouin zone is sufficient. The theoretical equilibrium lattice constant, determined by fitting the total energy of the GGA calculations as a function of volume to the Murnaghan equation of state [21], is 10.89 a.u. for the diamond phase which is only 1.9% larger than the experimental value of 10.69 a.u. The calculated bulk modulus is 76 GPa, in excellent agreement with the experimental value of 77 GPa at ambient pressure. In the β-Sn phase, the structural parameters were optimized at different pressures by minimizing the total energy. Besides using a single unit cell, additional XES calculations were performed for both the diamond-type and β-Sn phase using a 64 atoms ($2 \times 2 \times 2$) supercell. All atoms were treated as inequivalent with a 1s core hole created in one of the atoms. A 40 k points set was used in the self-consistent field (SCF) calculation and a more extensive 200 k points set was used in the XES calculations.

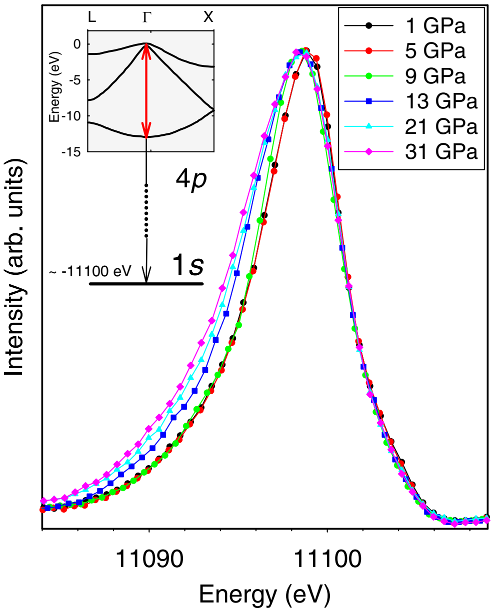

FIG. 1 (color online). Overview of valence-band emission spectra in Ge at selected pressures. We show the schematics of the transition from 4p to 1s states on the left. The 4p valence-band structure is adopted from [3], and the full bandwidth is indicated by the arrow (red online) in the inset. The details of the measurements and setup were reported in [31]. Spectra are normalized and shifted on the energy scale to match at the high-energy side of the peak. Emission spectra at 1, 5, and 9 GPa were collected from the semiconducting diamond-type phase and have nearly identical line shape, while the spectra at 13, 21, and 31 GPa from the metallic β-Sn phase demonstrate the linewidth which is increasing under pressure.

While the line shape of the emission spectra is modified by the response function of the spectrometer, we expect that the changes in the linewidth under pressure should not be affected appreciably by these broadening effects and can be traced back to the changes in the underlying band structure. We show theoretically calculated spectra in Fig. 2. To simulate core-hole lifetime effects we convoluted theoretical spectra with a $\Delta E = 1.96$ eV FWHM Lorentzian [22], and with a 1.5 eV FWHM Gaussian to take into account instrumental line broadening. The convoluted spectra shown in Fig. 2(c) demonstrate the increasing width of the valence band under pressure. The single unit cell calculations [Figs. 2(b) and 2(c)] show a sudden increase in the bandwidth from the diamond-type to β-Sn phase. However, instead of being nearly constant in the diamond-type phase the calculated Ge valence band width increases under pressure. We used several DFT functionals and found the results are independent of the functionals. We have also been very careful in the k point sampling and

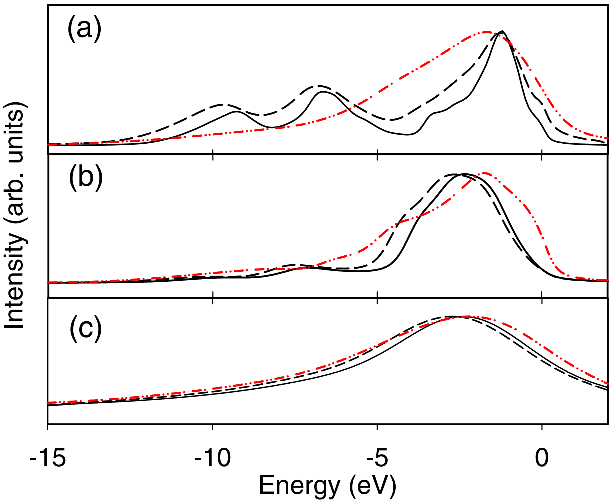

FIG. 2 (color online). Theoretically calculated valence-band region of the x-ray emission spectra. Black solid line—ambient pressure; black dashed line—diamond-type Ge at 9 GPa; red dash-dotted line—β-Sn Ge at 10 GPa. (a) XES calculated using a supercell method; (b) XES calculated from single unit cell; (c) theoretical spectra from Fig. 2(b) convoluted with Lorentzian (1.96 eV FWHM) and Gaussian (1.5 eV FWHM) to simulate effects of the core-hole lifetime and experimental resolution.

other technical parameters and found not much change. Figure 2(a) shows the XES spectra calculated from supercell model for diamond-type (using a very large 64 atoms unit cell) at 0 and 9 GPa, and for β-Sn at 10 GPa. We performed cluster calculations up to 836 atoms and see no changes from the band structure results. The trend is the same as in using the single unit cell electronic band structure [Figs. 2(b) and 2(c)], which is not surprising. We plot the change in the FWHM (ΔE) of the valence-band emission in Fig. 3. The experimental width of the valence-band emission line has increased by approximately 1 eV after the phase transition to the dense high-pressure β-Sn phase. In contrast to the theoretical results, in the low-pressure diamond-type phase the linewidth does not change with increasing pressure within the experimental uncertainty. The theoretical calculated linewidths are obtained from the single unit cell band structure calculations after convolution of the theoretical spectra according to the scheme shown in Fig. 2(c). We note that the experimental FWHM is about 6–7 eV, and derives most probably from p-like states at the top of the valence band. The calculated p-PDOS (projected density of states) of the diamond-type and the β-Sn phase at several pressures are shown in Fig. 4. The p-PDOS of diamond-type Ge shows three distinct bands with increasing p character at higher energy. The band at ~10 eV below the Fermi level has strong Ge 4s character and the highest energy band centered around 2.5 eV from the Fermi level composes of primarily Ge 4p states. Accordingly, the calculated XES using a single unit cell show a strong transition at around -2.5 eV with a distinct shoulder at -4 eV and two weaker bands at -7.5 and -10 eV. For the β-Sn Ge, both the calculated p-PDOS and the XES profile are much broader particularly for the high-energy band near the Fermi level. The calculated XES with the larger 64 atoms supercell show qualitatively similar patterns. However, in diamond-type Ge, the predicted intensities for the -7.5 and -10 eV bands are much stronger. In agreement with experiment, the width of the highest energy band of β-Sn Ge is significantly broader than for the diamond-type Ge. The XES profiles computed from the single unit cell calculations are in good agreement with experiment [Fig. 2(c)]. The theoretical XES obtained from the supercell calculations produced a similar trend but the agreement with experiment is less satisfactory. This is due to the large contribution of the intensities from the 8 to 10 eV below the Fermi level with large Ge 4s character which does not allow a comparison of the diamond-type and β-Sn theoretical results. It is likely that these transition intensities are overestimated by the supercell calculations.

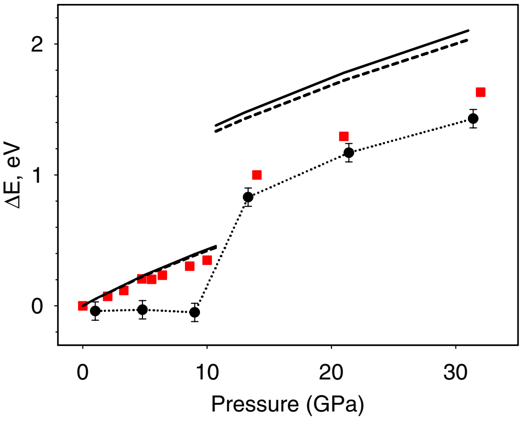

FIG. 3 (color online). Changes in the linewidth of the valence band in Ge under pressure. Circles with error bars—experiment; squares (red)—theory, single unit cell calculations. Solid line is an estimate for the half-width of the valence band in the free-electron approximation ($E_F/2$ for the free-electron gas); dashed line represents the free-electron calculation corrected according to the GWA results from Fig. 1 in Ref. [25].

A possible explanation for the pressure-independent linewidth of x-ray valence-band emission could be pursued with QP calculations taking into account many-body effects [10]. No such calculations were attempted in this work. It has been suggested from GW calculations on the homogeneous electron gas [23] that the experimentally observed reduction in the width of the valence band [24] in some free-electron-like metals with respect to its free-electron value is at least partly caused by many-body correlation effects. Theoretical calculations by Mahan and Sernelius [23] (the GW results without vertex corrections) predict relative valence-band narrowing, which becomes less pronounced at higher electronic densities [25]. In Fig. 3 the broadening of the free-electron-like valence band width is shown as a continuous line, and a dashed line represents corrections from GW calculations [23,25]. These results imply that in compressed Ge one would expect a negligible effect on the valence-band narrowing under compression due to many-body effects. The experimentally observed trend certainly does not follow these expectations. This discrepancy may be due to different nature of correlations in the semiconducting diamond-

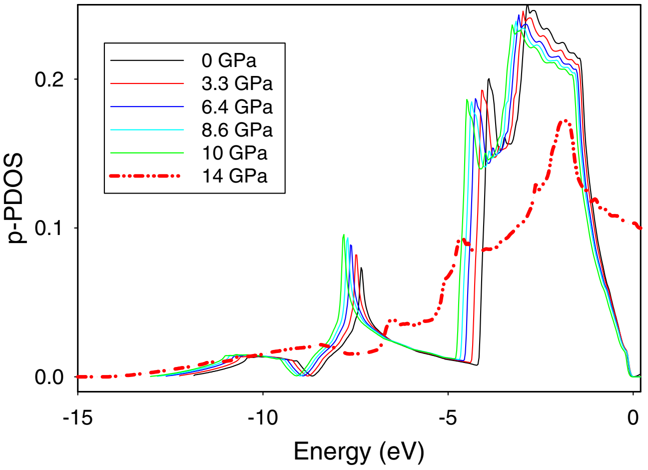

FIG. 4 (color online). Changes in the p-PDOS of the valence band of Ge under pressure. The width of the main peak (extending from 0 to -5 eV) is increasing under compression. See text for detailed discussion.

type Ge as compared to the simple alkali metals. Moreover, it has been shown [26,27] that the premise that the *GW* approximation (GWA) necessarily leads to band narrowing at $r_s > 1.6$ [25] is only true if one ignores self-consistency in solving the Dyson equation. Recent theoretical results [10] indicate that self-consistent calculations taking into account vertex corrections may be required for a fundamental description of the entire valence QP band structure of Ge (and Si) within 0.1 eV accuracy; moreover, such an accuracy may even require the inclusion of mechanisms beyond the GWA [28]. It is quite possible that these mechanisms can be tested using our data on the valence-band behavior in compressed Ge.

In summary, the reported measurements demonstrate feasibility of studies of the valence-band structure in compressed semiconductor. Theoretically calculated pressure-induced changes in the valence band width within the DFT framework are in good agreement with the experiment in the metallic β-Sn phase of Ge above 10 GPa. However, in the semiconducting diamond-type phase below 10 GPa the experimental valence band width does not show any of the broadening effects predicted theoretically. It is generally believed that DFT methods are sufficient to describe band structure of semiconducting Ge and Si; however, our results indicate that valence-band electronic structure could not be described satisfactorily within the DFT framework. We believe that electronic correlation effects neglected in DFT are responsible for the observed behavior. Further QP calculations within the self-consistent *GW* approximation or beyond may be required to understand the experimental findings. Future XES experiments may provide further important information on the valence band changes through the high-pressure Cmca and hcp phases of Ge [29]. Experiments using resonant inelastic x-ray scattering technique at the *K* edge of Ge [30] may also provide more detailed information on the valence-band structure of compressed Ge.

HPCAT is supported by DOE, NSF, and the W. M. Keck Foundation. V. V. S. acknowledges financial support from the Department of Energy under Grant No. DE-FG02-02ER45955. We thank E. Shirley for his comments and input during the early stages of this work, and the HPCAT staff D. Häusermann, M. Somayazulu for technical assistance.

---

*Now at Lawrence Livermore National Laboratory, 7000 East Avenue, Livermore, CA 94550.

†Now at the Department of Physics and Engineering Physics, University of Saskatchewan, Saskatoon, S7N 5E2, Canada.

‡Now at National High Pressure Laboratory, Jilin University, Changchun China.

[1] P. Hohenberg and W. Kohn, Phys. Rev. **136**, B864 (1964).
[2] W. Kohn and L. J. Sham, Phys. Rev. **140**, A1133 (1965).
[3] M. Hybertsen and S. G. Louie, Phys. Rev. Lett. **55**, 1418 (1985); Phys. Rev. B **34**, 5390 (1986).
[4] R. W. Godby, M. Schlüter, and L. J. Sham, Phys. Rev. Lett. **56**, 2415 (1986); Phys. Rev. B **37**, 10 159 (1988).
[5] J. E. Northrup, M. S. Hybertsen, and S. G. Louie, Phys. Rev. Lett. **59**, 819 (1987); Phys. Rev. B **39**, 8198 (1989); For an alternative interpretation, see G. D. Mahan and B. E. Sernelius, Phys. Rev. Lett. **62**, 2718 (1989).
[6] M. Rohlfing, P. Kruger, and J. Pollmann, Phys. Rev. B **48**, 17 791 (1993).
[7] E. L. Shirley, Phys. Rev. B **54**, 7758 (1996).
[8] W. Ku and A. G. Eguiluz, Phys. Rev. Lett. **82**, 2350 (1999).
[9] H. Yasuhara, S. Yoshinaga, and M. Higuchi, Phys. Rev. Lett. **83**, 3250 (1999).
[10] W. Ku and A. G. Eguiluz, Phys. Rev. Lett. **89**, 126401 (2002).
[11] A. R. Goñi, K. Syassen, and M. Cardona, Phys. Rev. B **39**, 12 921 (1989).
[12] J. A. Bearden, Rev. Mod. Phys. **39**, 78 (1967).
[13] U. von Barth and G. Grossmann, Phys. Rev. B **25**, 5150 (1982).
[14] W. Ku, A. G. Eguiluz, and E. W. Plummer, Phys. Rev. Lett. **85**, 2410 (2000).
[15] H. Yasuhara, S. Yoshinaga, and M. Higuchi, Phys. Rev. Lett. **85**, 2411 (2000).
[16] G. L. Bir and G. E. Pikus, *Symmetry and Strain Induced Effects in Semiconductors* (Wiley, New York, 1974).
[17] G. A. Samara and C. A. Barnes, Phys. Rev. B **35**, 7575 (1987).
[18] P. Blaha, K. Schwarz, G. K. H. Madsen, D. Kvasnicka, and J. Luitz, *WIEN2K, An Augmented-Plane-Wave + Local Orbitals Program for Calculating Crystal Properties* (Karlheinz Schwarz, Technical University of Wien, Vienna, 2001), ISBN 2-9501031-1-2.
[19] J. P. Perdew and K. Burke, Int. J. Quantum Chem. **S57**, 309 (1996); J. P. Perdew, K. Burke, and M. Ernzerhof, Phys. Rev. Lett. **77**, 3865 (1996).
[20] J. P. Perdew and Y. Wang, Phys. Rev. B **45**, 13 244 (1992).
[21] F. D. Murnaghan, Proc. Natl. Acad. Sci. U.S.A. **30**, 244 (1944).
[22] M. O. Krause and J. H. Oliver, J. Phys. Chem. Ref. Data **8**, 329 (1979).
[23] G. D. Mahan and B. E. Sernelius, Phys. Rev. Lett. **62**, 2718 (1989).
[24] P. H. Citrin, G. K. Wertheim, T. Hashizume, F. Sette, A. A. MacDowell, and F. Comin, Phys. Rev. Lett. **61**, 1021 (1988).
[25] G. E. Engel and Warren E. Pickett, Phys. Rev. B **54**, 8420 (1996).
[26] B. Holm and U. von Barth, Phys. Rev. B **57**, 2108 (1998); A. G. Eguiluz and W.-D. Schöne, Mol. Phys. **94**, 87 (1998).
[27] W.-D. Schöne and A. G. Eguiluz, Phys. Rev. Lett. **81**, 1662 (1998).
[28] We have performed *GW* calculations on the FCC phase and found the same trend as predicted by the LDA calculations. We acknowledge J. A. Soininen for the *GW* calculations.
[29] K. Takemura, U. Schwarz, K. Syassen, M. Hanfland, N. E. Christensen, D. L. Novikov, and I. Loa, Phys. Rev. B **62**, R10603 (2000).
[30] Y. Nisikawa, M. Usuda, J. Igarashi, H. Shoji, and T. Iwazumi, J. Phys. Soc. Jpn. **73**, 970 (2004).
[31] V. V. Struzhkin, R. J. Hemley, H.-k. Mao, Yu. A. Timofeev, and M. I. Eremets, Hyperfine Interact. **128**, 323 (2000).